HHS Public Access

Author manuscript

Sci Signal. Author manuscript; available in PMC 2018 March 05.

Published in final edited form as:

Sci Signal. ; 10(495): . doi:10.1126/scisignal.aam7703.

Bacterial D-Amino Acids Suppress Sinonasal Innate Immunity Through Sweet Taste Receptors in Solitary Chemosensory Cells

Robert J. Lee[1,2,†], **Benjamin M. Hariri**[1], **Derek B. McMahon**[1], **Bei Chen**[1], **Laurel Doghramjii**[1], **Nithin D. Adappa**[1], **James N. Palmer**[1], **David W. Kennedy**[1], **Peihua Jiang**[3], **Robert F. Margolskee**[3], and **Noam A. Cohen**[1,3,4,†]

[1]Department of Otorhinolaryngology—Head and Neck Surgery, University of Pennsylvania Perelman School of Medicine

[2]Department of Physiology, University of Pennsylvania Perelman School of Medicine

[3]Monell Chemical Senses Center

[4]Philadelphia VA Medical Center Surgical Service

Abstract

In the upper respiratory epithelium, bitter and sweet taste receptors present in solitary chemosensory cells influence antimicrobial innate immune defense responses. Whereas activation of the bitter taste receptor (T2R) stimulates surrounding epithelial cells to release antimicrobial peptides, activation of the sweet taste receptor (T1R) in the same cells inhibits this response. It is thought that this mechanism exists to control the magnitude of antimicrobial peptide release based upon the sugar content of airway surface liquid. We hypothesized that D-amino acids, which are produced by various bacteria and activate T1R in taste receptor cells in the mouth, may also activate T1R in the airway. Here, we show that both the T1R2 and T1R3 subunits of the sweet taste receptor (T1R2/3) are present in the same chemosensory cells of primary human sinonasal epithelial cultures. Respiratory isolates of *Staphylococcus* species, but not *Pseudomonas aeruginosa*, produced at least two D-amino acids that activate the sweet taste receptor. In addition to inhibiting *P. aeruginosa* biofilm formation, D-amino acids derived from *Staphylococcus* inhibited T2R-mediated signaling and defensin secretion in sinonasal cells by activating T1R2/3. D-amino acid–mediated activation of T1R2/3 also enhanced epithelial cell death during challenge with *Staphylococcus aureus* in the presence of the bitter-receptor–activating compound denatonium benzoate. These data establish a potential mechanism for interkingdom signaling in the airway mediated by bacterial D-amino acids and the mammalian sweet taste receptor in airway chemosensory cells.

[†]Co-corresponding authors: rjl@mail.med.upenn.edu (R.J.L.) and cohenn@uphs.upenn.edu (N.A.C.).

Author Contributions: R.J.L. and N.A.C. conceived and designed the study and wrote the paper. R.J.L., B.M.H., D.B.M., and B.C. performed experiments. N.A.C., L.D., N.D.A., J.N.P., and D.W.K. recruited patients for the study, collected tissue samples, and maintained clinical databases. R.F.M. and P.J. contributed reagents and contributed to intellectual design. All authors reviewed and approved of the final manuscript.

Competing Interests: The authors declare that no conflicts or competing interests exist.

Introduction

The nose and sinuses are the front line of respiratory defense (1). When sinonasal immunity fails, it can result in chronic rhinosinusitis (CRS), a debilitating disease affecting >10% of Americans and accounting for ~$8 billion dollars of annual direct healthcare costs (2–4). First line therapy for bacterial rhinosinusitis involves antibiotics; rhinosinusitis accounts for 1 in 5 antibiotic prescriptions for adults in the US, making it a major contributor to the rising crisis of antibiotic resistance (5–7). There is a critical need to better understand the regulation of endogenous sinonasal immune responses to identify novel therapeutic targets that could treat CRS without the use of antibiotics to avoid selective pressures for resistance. We previously showed that sinonasal solitary chemosensory cells (SCCs), a recently identified cell type in the upper airway, stimulate secretion of antimicrobial peptides (AMPs) through bitter taste receptors (T2Rs) (8). T2Rs, originally identified on the tongue (9, 10), are found in many tissues throughout the body (11–13). T2Rs are activated by toxic plant products such as alkaloids as well as bitter bacterial products, such as acyl-homoserine lactone (AHL) quorum sensing molecules (8, 13–18). SCCs, a specific cell type found at a frequency of ~1:100 in the upper airway and which expresses both bitter and sweet taste receptors, were first described in fish (19) and later in alligators (20), rodents (21–23), and humans (8, 24). SCCs are defined by expression of taste-signaling components, including bitter receptors (T2Rs), sweet receptors (T1R2/3) and Gα-gustducin (8, 21–24). Activation of T2Rs in human sinonasal SCCs stimulates propagation of a calcium wave to the surrounding epithelial cells, causing release of AMPs, including β-defensins, that kill bacteria (8).

This mechanism is inhibited by activation of sweet taste receptors (T1Rs) (25), which are localized within the same SCCs as the bitter taste receptors (8). SCC responses stimulated by the bitter T2R agonist denatonium are blocked in a dose-dependent fashion by sugars such as glucose and sucrose, as well as the non-metabolizable artificial sweetener sucralose (8). This inhibition is blocked by the T1R2/3 (T1R receptor containing T1R2 and T1R3 subunits) antagonists lactisole (26–28) and amiloride (29), but not by inhibitors of glucose transporters (8). Glucose tonically leaks across the epithelium into the airway surface liquid (ASL) through paracellular pathways, but re-uptake through apical glucose transporters in the healthy state maintains ASL glucose around 0.5 mM or less, which is approximately 10-fold less than fasting serum concentration (30–32). However, such low glucose concentrations are nonetheless sufficient to partially activate T1R2/3 in human nasal SCCs (8). We have hypothesized that T1R2/3 acts as a rheostat to control the magnitude of the antimicrobial peptide response depending on ASL glucose concentrations, desensitizing SCC T2Rs to bitter compounds during colonization. This desensitization would be relieved when bacterial numbers increase enough to cause depletion of ASL glucose though bacterial glucose consumption, signaling the onset of a *bona fide* infection (8).

Although this hypothesis requires further validation, another mechanism by which airway T1R2/3 receptors may be activated is through bacterial production of D-amino acids, several of which activate the sweet taste receptor (26, 33). Life has evolved to predominately utilize L-amino acids as protein building blocks, but bacteria produce a diverse array of D-amino acids used as cell wall structural components and possibly intercellular signals. The

racemase activity of bacteria and their resulting ability to interconvert and metabolize both D- and L-amino acids have been proposed to be responsible for maintaining the relatively low D-amino acid:L-amino acid ratio found on earth (34). The gram-negative bacterium *Vibrio cholera* and the gram-positive bacterium *Bacillus subtilis* produce D-amino acids, which may reduce peptidoglycan synthesis and influence cell wall remodeling (35).

D-amino acids may stimulate biofilm disassembly in *B. subtilis* (36) and inhibit biofilm formation of *Pseudomonas aeruginosa* (37, 38), *Staphylococcus aureus* (39) (40), and *Staphylococcus epidermidis* (41) as well as cause dispersal or detachment of cells from single-species and multi-species biofilms containing *P. aeruginosa* (42), *S. epidermidis* (41), or *Staphylococcus aureus* (43, 44). D-amino acids may inhibit adhesion of bacterial cells to one another (45, 46). However, other studies starkly conflict with these results and suggest D-amino acids at 1 mM do not inhibit biofilm growth in *S. aureus*, *B. subtilis*, or *S. epidermidis* (47). Effects of D-amino acids on *B. subtilis* may be simply due to toxic effects of inhibition of protein synthesis (48). Others have reported that mixtures of D-amino acids (49) or combinations of D-amino acids with antibiotics (50) may be more effective against biofilm formation than individual D-amino acids. Interpretation of these studies is complicated due to differences in strains, biofilm assays (for example, microtiter plate vs. flow-cell), and the dosage of specific D-amino acids used (51).

Regardless of the controversy over the mechanism(s) of action of D-amino acids on the bacteria themselves, both gram-negative and gram-positive bacteria produce various D-amino acids at relatively high concentrations (in the high-μM to low-mM range) (35, 36, 52). This range is predicted to be sufficient to activate the sweet taste receptor (33, 53) on the airway epithelial SCCs that produce T1R2/3. We hypothesize that certain D-amino acids produced by bacteria may play an important role in host-pathogen interactions in the sinonasal cavity by activating the sweet taste receptor in SCCs, and thus we sought to study the effects of sweet-receptor–activating D-amino acids on upper respiratory epithelial cells and on the physiology of respiratory bacteria. Our goal was to test the effects of bacterially-produced D-amino acids on airway epithelial innate immune responses to understand how they may influence host-pathogen interactions in the upper respiratory tract.

RESULTS

Sinonasal solitary chemosensory cells produce the T1R2 and T1R3 subunits of the sweet taste receptor

The canonical sweet taste receptor is composed of Tas1R2 (T1R2) and Tas1R3 (T1R3) subunits (54). A closely related subunit, Tas1R1 (T1R1), also combines with T1R3 to form the umami receptor (Fig. 1A–B). These proteins are found only in vertebrates and are members of the class C family of G protein–coupled receptors (GPCRs), which also includes metabotropic glutamate receptors as well as several receptors that detect amino acids and small peptides, including V2R pheromone receptors (Fig. 1A and fig. S1, Table S1) (54). The evolution of T1Rs from ancestral receptors for amino acids and peptides likely explains the reactivity of these receptors to certain amino acid isoforms. Typically, the umami receptor (T1R1/3, formed by the association of T1R1 and T1R3 subunits) detects L-isomer (savory) amino acids, and the sweet receptor (T1R2/3, formed by the association of

T1R2 and T1R3) detects certain D-isomers of amino acids in addition to various sugars, including sucrose, glucose, and fructose (55), as well as several known sweet peptides, such as monellin (56).

When primary human sinonasal cells were grown in air-liquid interface (ALI) cultures, these cultures contained SCCs, which were identified by morphological criteria and production of both bitter and sweet taste receptors as previously described in mouse (57) and human (8, 58). SCCs are found at an approximate frequency of about 1 in 100 cells in the mouse sinonasal epithelium (57). Although we previously reported that human SCCs produce both T1R2 and T1R3 along with the bitter taste receptor T2R47, we did not determine whether the same SCC produces both T1R2 and T1R3 together, which would be required for formation of the canonical sweet taste receptor, T1R2/3. Here we used direct labeling of SCCs using antibodies recognizing both T1R2 and T1R3 subunits. All SCCs observed in these cultures produced both T1R2 and T1R3 (Fig. 1C, fig. S2). We did not observe any SCCs in which only T1R2 or T1R3 was present alone. When co-staining was done with T2R47 and T1R2 or T1R3, T2R47-positive cells were always observed to produce T1R2 or T1R3. Based on these and our previous observations from human (8) and other observations of mouse SCCs (17, 21, 57), we conclude that sinonasal SCCs produce both bitter taste receptors (such as T2R47) and both subunits of the T1R2/3 receptor. However, our data do not rule out the existence of a distinct subset of SCCs that expresses neither T1R2 nor T1R3.

T1R2/3-activating D-amino acids are produced by bacteria cultured from the human sinonasal cavity

We hypothesized that D-amino acids produced by bacteria may impair the ability of SCCs to stimulate innate immune responses by activating T1R2/3. It is important to note here that in this study, we are not measuring "sweetness," which is a complex gustatory sensation, but rather are looking at activation of the T1R2/3 receptor. Thus, instead of referring to these amino acids as "sweet" as in many psychophysics studies (59, 60), we refer to them here as "T1R2/3-activating" amino acids, as demonstrated in previous molecular experiments (26, 33). We measured the abundance of several D-amino acids known to activate the T1R2/3 receptor (D-Ile, D-Phe, and D-Leu; (26, 33)) in bacterial cultures grown from human sinonasal swabs from chronic rhinosinusitis patients. Not all D-amino acids activate the sweet taste receptor; an example is D-proline, which does not activate T1R2/3 and is perceived as bitter (61). Thus, we specifically focused on D-Ile, D-Phe, and D-Leu, which are known to activate T1R2/3. Because these samples came from human patients, they were not strictly single-species cultures, so we determined the predominant microorganisms present in each culture. These included *S. aureus*, coagulase-negative *Staphylococcus* (likely primarily *S. epidermidis*), *P. aeruginosa*, and *A. fumagatus*. We classified these cultures by the predominant species present in the culture, but other species were also present in each culture at lower abundance. Cultures in which either *S. aureus* or coagulase-negative *Staphylococcus* was predominant contained D-Phe and D-Leu, whereas cultures in which *P. aeruginosa* or *A. fumagatus* were predominant did not (Fig. 2A).

D-amino acids reduce *P. aeruginosa* biofilm formation and swarming

To determine whether the D-amino acids present in clinical microbiologic cultures might affect the growth of bacteria, we grew wild-type *P. aeruginosa* strain PAO1 and methicillin-resistant *S. aureus* (MRSA) strain M2 in filter-sterilized conditioned medium (CM) from sinonasal clinical cultures. CM from cultures in which *S. aureus* was predominant, but not CM from cultures in which *P. aeruginosa* was predominant, reduced biofilm formation by *P. aeruginosa* strain PAO1 (Fig. 2B). MRSA M2 biofilm formation was not affected by CM from either *S. aureus*-predominant or *P. aeruginosa*-predominant cultures. When a clinical MRSA strain and *P. aeruginosa* PAO1 biofilms were grown in medium supplemented with varying concentrations of D-Phe, D-Leu, and D-Tyr (another D-amino acid previously shown to be produced by *P. aeruginosa* and activate T1R2/3 (35)), we found that *P. aeruginosa* PAO1 exhibited a 10-fold lower IC_{50} than did MRSA as well as a higher maximum inhibition of biofilm formation (Fig. 2C), suggesting that *P. aeruginosa* PAO1 has a greater sensitivity to the biofilm-inhibitory effects of D-amino acids produced by *Staphylococcus* species. L-amino acids supplemented at the same concentrations had no effect on biofilm formation (Fig. 2C). Whether these concentrations translate to in vivo D-amino acid production remains to be determined.

We noted that planktonic cultures of *P. aeruginosa* (wild-type PAO1 or ATCC27853) grown in the presence of two T1R2/3-activating D-amino acids (D-Phe + D-Leu) were less blue-green than when cultured in the absence of these D-amino acids (Fig. 3A). This was due at least in part to a reduction in the production of pyocyanin, a secreted toxic secondary metabolite (Fig. 3B–C). As a control, a strain deficient in AHL quorum sensing (PAO-JP2; Δ*lasI*, Δ*rhlI*), which produces very little pyocyanin at baseline (Fig. 3B), was unaffected by the presence of D-Phe or D-Leu (Fig. 3C). Because biofilm formation and pyocyanin production are under the control of the AHL quorum-sensing system, we also tested swarming motility in *Pseudomonas*, which is likewise controlled by quorum sensing. Swarming is important for bacterial spreading and biofilm formation (62) and requires flagellar function and rhamnolipid production (62, 63). Swarming is evidenced by a characteristic irregular radiation of cells from a spot on semi-solid high-density agar plates that mimic gelatinous viscous surfaces like a mucosal membrane (62). In contrast, swimming on low agar plates, which reflects random twitching motility, results in a more even diffusive colony spread (Fig. 3D). Swarming was markedly inhibited in the presence of D-Phe and D-Leu, but not in the presence of L-Phe and L-Leu for PAO-GFP (a derivative of PAO-1) and ATCC 27853. The presence of either L- or D-amino acids did not affect swarming of PAO-JP2 (Fig. 3E). The above data support some role of D-amino acids in inhibition of quorum-sensing and biofilm formation in vitro.

Because D-amino acids have been implicated in bacterial biofilm dispersal as well as cell wall remodeling of some bacteria, we tested the effects of T1R2/3-activating D-amino acids on dispersion of microcolonies of PAO-GFP grown on glass coverslips (fig. S3), low-salt sensitivity of PAO-1 (fig. S4), and antibiotic resistance of PAO-GFP and ATCC27853 (fig. S5). We observed no differences in any of these parameters between bacteria exposed to D- or L-amino acids. Our negative data suggest that these T1R2/3-activating D-amino acids do not affect *P. aeruginosa* dispersion or cell wall integrity.

T1R2/3-activating D-amino acids affect innate immune responses of sinonasal cells by modulating the T1R2/3 receptor

We next tested the effects of the T1R2/3-activating D-amino acids D-Phe and D-Leu on host cell innate immune responses. We examined the effect of D- and L-isomers of Phe and Leu on T2R-mediated calcium responses of human SCCs grown in air-liquid interface (ALI) cultures. This culturing method is a standard in vitro model of the airway epithelium that mimics the morphology of the in vivo airway epithelium and includes ciliated cells, goblet cells, and SCCs (8, 14, 64–66). ALI cultures grown in physiological concentrations of basolateral glucose (5 mM or 90 mg/dl) produce airway surface liquid (ASL) containing ~0.3–0.5 mM glucose, which is similar to the concentration of glucose in control nasal fluid samples (8). This glucose concentration, which results from transepithelial leak of basolateral glucose through paracellular pathways balanced by cellular re-uptake of glucose through apical GLUT transporters (30, 31), is sufficient to slightly attenuate T2R Ca^{2+} responses in SCCs (8). For this reason, cultures were thoroughly washed immediately before experiments to remove any residual ASL glucose that may influence the cells.

As previously reported (8), the T2R agonist denatonium benzoate stimulated Ca^{2+} responses from SCCs that were inhibited dose-dependently by the presence of apical glucose (0.5–5 mM). The sweet taste receptor antagonists lactisole (27, 28) and gymnemic acid (67, 68) blocked glucose-mediated inhibition of SCC calcium responses (Fig. 4A). When SCCs were exposed to D-Leu or D-Phe, but not L-Leu or L-Phe, they likewise exhibited reduced denatonium-stimulated Ca^{2+} responses (Fig. 4B) that were also reversed by lactisole. We previously showed that these SCC calcium responses, summarized in (Fig. 4C), drive antimicrobial peptide secretion from surrounding epithelial cells in response to T2R receptor stimulation (8). The D-Leu and D-Phe suppression of denatonium-induced calcium signaling suggest that D-Leu and D-Phe have effects on SCC signal transduction upstream of antimicrobial peptide release, as we previously reported for sugars and artificial sweeteners acting through the sweet taste receptor (8). The decrease in SCC Ca^{2+} signaling elicited by D-Leu and D-Phe also resulted in reduced β-defensin 1 (BD1) secretion, which was likewise reversed by lactisole (Fig. 4D). D-Phe and D-leu also reduced Ca^{2+} responses in cultured nasal septum ALIs from wild-type but not T1R3 knockout mice (fig. S6), supporting that this reduction occurs through the sweet taste receptor.

We next tested the hypothesis that T1R2/3-activating D-amino acids impair epithelial defense by examining the effects of MRSA bacterial co-culture on cell viability in sinonasal ALI cultures in the presence and absence of these secreted D-amino acids. We examined host cell death following incubation of the cells with the laboratory strain MRSA-M2, by determining the the proportion of live and dead cell staining with Syto9, a fluorescent compound that labels the nuclei of both live and dead cells, and propidium iodide (PI), a fluorescent compound that labels the nuclei only of dead or dying cells. We estimated the number of live and dead cells by measuring the relative areas of Syto9 and PI staining, respectively, using fluorescence microscopy. Representative images are shown in (Fig. 5A) with quantification of staining in (Fig. 5B). In the absence of bacteria, ALI cultures exhibited no detectable cell death (Fig. 5A, upper left), evidenced by a lack of PI staining. Incubation with MRSA ± D-amino acids (D-Phe + D-Leu; 200 μM) induced widespread cell

death (Fig. 5A). that was slightly reduced with lactisole compared to incubation with MRSA + D-amino acids alone (Fig. 5A top row, quantified in Fig. 5B). However, addition of the T2R agonist denatonium resulted in fewer dead cells in cultures exposed to MRSA than did treatment with MRSA alone (Fig. 5A), likely because of antimicrobial peptides secreted in response to denatonium activation of SCC T2Rs. The addition of D-amino acids exacerbated cell death under these conditions (Fig. 5A–B), which was reversed by lactisole or gymnemic acid 2 (GA2) (Fig. 5A, middle row, quantified in Fig. 5B). This suggests that DAA activation of T1Rs inhibits the protective T2R-activated antimicrobial peptide response, reducing epithelial defense.

To demonstrate the relevance of this effect to clinically-produced levels of D-amino acids, we tested the effects of MRSA strain M2 CM from 24 hr. overnight cultures. MRSA CM blocked the protective effects of denatonium, resulting in cell death, but had no effect in the presence of lactisole (Fig. 5A, bottom row, quantified in Fig 5B). Treatment of patient-derived ALI cultures with PAO1 CM had no effect (Fig. 5A, bottom row, quantified in Fig 5B), suggesting that *Staphylococcus*, but not *Pseudomonas*, CM contains molecules, likely D-amino acids, that activate T1R to a level that reduces sinonasal innate immune responses by inhibiting antimicrobial peptide release,

DISCUSSION

The role of the T1R2/3 sweet taste receptor in sinonasal SCCs may have pathophysiological consequences in patients with diabetes mellitus, chronic rhinosinusitis, or cystic fibrosis, all of whom have been reported to have increased ASL glucose concentrations (8, 30, 69–71). In control patients, nasal ASL glucose is low (<0.5 mM), which is similar to in vitro observations of ALI cultures grown in physiological (5 mM, or 90 mg/dl) basolateral glucose (8). This amount of glucose only minimally attenuates SCC T2R responses. However, in patients with epithelial damage due to inflammatory disease, nasal ASL glucose is much higher (~1–2 mM), which significantly inhibits SCC T2R responses (8). Thus, increased ASL glucose secondary to disease may have inhibitory effects on epithelial innate immunity. Here, we show a further relevance of this mechanism to disease pathogenesis by demonstrating that sinonasal SCC T1R2/3 can be activated by bacterial D-amino acids. The data presented here show that clinically relevant respiratory gram-positive *Staphylococcus* bacteria produce at least two T1R2/3-activating D-amino acids. Effects of D-amino acids may be magnified in combination with already high ASL glucose found in patients with sinonasal disease.

Because these D-amino acids have some effects on *P. aeruginosa,* this may be an important mechanism of bacterial crosstalk in the human airways. Interestingly, we found that D-amino acids were secreted by both *S. aureus* and *S. epidermidis*, generally considered to be non-pathogenic components of the normal respiratory flora (72). Although *S. aureus* plays an important role in chronic rhinosinusitis (73), it is considered an opportunistic pathogen because it is also a frequent colonizer of healthy sinuses (74–76). The secretion of D-amino acids may be a mechanism by which *Staphylococcus* strains suppress *P. aeruginosa* virulence, thus supporting a role for commensal *Staphylococcus* in preventing pathogenic growth of *P. aeruginosa* in the airways. Further studies are needed to understand if this

mechanism occurs at physiological concentrations of D-amino acids and whether it is involved in competition or growth coordination.

We also show that D-amino acids produced by *Staphylococcus* bacteria can suppress sinonasal SCC innate immune responses through activation of T1R and inhibition of AMP secretion. This may be a mechanism by which *Staphylococcus* species protect themselves from eradication and allow them to colonize human airways. More work is needed to determine whether the presence of D-amino acids in nasal mucus in infected patients is a potential biomarker of *Staphylococcus*-driven infections and whether T1R sweet receptor antagonists (for example, lactisole or gymnemic acid) are useful topical therapeutics in *S. aureus*–infected patients.

It has long been known that the innate and adaptive immune systems utilize pattern recognition receptors (PRRs) to detect conserved bacterial and viral components, such as toll-like receptor 4 (TLR4)–mediated recognition of bacterial lipopolysaccharide (77). Our previous work (8, 14) and that of others (15–17) has demonstrated that T2Rs serve in an immune role similar to PRRs beyond their already established role on the tongue (25). The data here demonstrate that the T1R2/3 heterodimer also functions much like a PRR by recognizing bacterial D-amino acids, implicating D-amino acids in interkingdom signaling. However, in contrast to TLRs and T2Rs, activation of T1Rs suppresses innate immune responses. We do not yet know whether this provides a host benefit in vivo, for instance in the prevention of activation of immune responses against commensal bacteria, or if this is a mechanism by which pathogenic bacteria evade detection. One study has linked several *TAS1R* polymorphisms to increased risk for developing CRS (78). Because the sweet taste receptor has multiple ligand binding sites (26), further research is needed to determine if these polymorphisms affect the T1R response to D-amino acids. Because T1Rs are also present on other cell types throughout the body (11, 79), they may serve as PRR-like receptors that either suppress or stimulate innate immunity outside the airway.

MATERIALS AND METHODS

Reagents and Solutions

Fluo-4 and LIVE/DEAD® *Bac*Light® Bacterial Viability Kit were purchased from Thermo Fisher Scientific. Lactisole (Cypha) was from Domino Foods, Inc. Purified gymemic acid 2 was from Four, LLC. β-defensin 1 ELISA development kit was from Peprotech and was carried out according to the manufacturer's instructions. Unless specified, all other reagents were from Sigma-Aldrich. Antibodies recognizing T1R2 (Abcam ab65417; RRID:AB_2200812) and T1R3 (Abcam ab65419; RRID:AB_1139947) for immunofluorescence, which were validated by Western blot in a previously published study (80) as well as in HEK293T cells transfected with T1R2 or T1R3 (fig. S2), were used at 1:100. Antibody against T2R47 (Abcam ab65516; RRID:AB_1143241) was validated in our previous study (8). Antibody specific for β-Tubulin IV was from Abcam (ab11315; RRID:AB_297919; mouse monoclonal; used at 1:250).

Phylogenetic Tree Construction

Evolutionary history was inferred using a Maximum Likelihood Jones-Taylor-Thornton (JTT) matrix-based model (81) on protein sequences obtained from GenBank and aligned with Muscle in MEGA6 (118 amino acid sequences; positions containing gaps and missing data were eliminated, resulting in 117 positions in the final dataset) (82). The full highest log likelihood tree (−12115.8392) is shown in fig. S1. The percentage of trees in which the associated taxa clustered together is shown next to the branches. Initial tree(s) for the heuristic search were obtained by applying the Neighbor-Joining method to a matrix of pairwise distances estimated using a JTT model. Branch lengths reflect the number of substitutions per site.

Bacterial Culture

Bacterial strains PAO1 (ATCC), MRSA M2 (83), ATCC 27853 (Boston 41501), PAO-GFP (gentamycin^r), and PAO-JP2 (Δ*lasI*, Δ*rhlI*; Tc^r, $HgCl_2^r$) (84, 85) were grown as previously described (8, 14). Patient sinonasal microbiology cultures were collected using BBL CultureSwab Plus transport system (Becton, Dickinson, and Co., Sparks MD USA), grown overnight in lysogeny broth (LB) media, and speciated by the Philadelphia VA Medical Center microbiological laboratory. Detection of D-amino acids from bacterial cultures was performed by the Children's Hospital of Philadelphia Metabolomics Core, using liquid chromatography followed by tandem mass spectrometry (LC-MS/MS) to detect D- and L-form stereo-isoforms of Phe, Leu, Ile, and Trp. Microbiological cultures isolated from human sinonasal swabs were grown for 24 hrs at 37 °C in LB medium, followed by normalization of turbidity to 0.5 MacFarland. Sweet D-amino acid production was determined via liquid chromatography and tandem mass spectrometry (LC-MS/MS).

Biofilm assays were performed using crystal violet staining in a 96 well plate as previously described (86). Briefly, bacteria were normalized to 0.5 McFarland in LB or conditioned media and then 100 μL was aliquoted to 96 well plates containing 100 μL of 0.9% saline with the desired D- or L-amino acid(s) if applicable. Due to the poor solubility of Tyr, the maximum concentration of L-Tyr or D-Tyr in these experiments was 0.1 mM. In some assays, L-Phe and L-Leu or D-Phe and D-Leu were increased above 0.1 mM as indicated in the figures, but the concentration of L-Tyr or D-Tyr was not increased beyond 0.1 mM. After incubation for 48 hrs at 37 °C, microtiter plates were washed 3 times with distilled water, followed by staining with 1% crystal violet at room temperature for approximately 30 min. After a second round of washing, biofilm mass and crystal violet were solubilized by incubation in 30% acetic acid for 30 min with shaking, and read on a plate reader at 590 nm. Absorption spectra of bacterial culture supernatants were measured on a Tecan Spark 10M plate reader.

Pyocyanin extraction was carried out as previously described (87). Briefly, 8ml of supernatant from an overnight culture (grown in cation-adjusted Mueller-Hinton broth, normalized to OD600 = 1) was mixed with 3 ml of chloroform. After vortexing and centrifugation, pyocyanin was extracted from the resulting organic chloroform phase with 1 ml of 0.2 N HCl, with absorbance of the acidified pyocyanin read at 520 nm in a plate reader (Biorad). All values were blanked to LB that had undergone the same extraction procedure.

Relative concentrations of pyocyanin are shown because we are measuring relative inhibition and did not standardize to purified pyocyanin. However, raw pyocyanin concentration can be estimated using the molar extinction coefficient of acidified pyocyanin (pyocyanin in μg/ml = OD520 × 17.072 and pyocyanin molecular weight = 210.23, as previously described (87)). Pyocyanin concentration in PAO1 cultures grown to OD_{600} ~1 in peptone broth were previously reported to be ~60 μM (88). We estimate pyocyanin in PAO1 cultures grown to OD_{600} = 1 in Mueller Hinton broth here to be 23 μM.

Bacterial swarming and swimming assays were performed as previously described (62, 89, 90). Plates contained (per 500 ml of M9 minimal media): 1 g glucose, 2.5 g casamino acids, and 60 mg MgSO4 plus 1.5 g (0.3% final concentration) or 4 g (0.8% final concentration) agar for swimming or swarming, respectively. Filter sterilized solutions of L- or D-amino acids were added after autoclaving to prevent any heat-induced degradation. After spotting of 10 μL bacteria (adjusted to OD_{600} = 1), plates were allowed to dry for 2 hr at room temperature and incubated over night at 37 °C. Antibacterial resistance tests were performed under the supervision of the Philadelphia VA Medical Center microbiological laboratory according to procedures previously outlined (91). Bacteria were normalized to 0.5 McFarland before plating on Mueller-Hinton agar plates coated with D- or L-amino acids (2 mM each in ddH_2O applied with sterile swabs) prior to application of a broad spectrum of antibiotics against gram-negative bacteria as indicated. Antibiotic resistance experiments were performed under the supervision of Dr. L. Chandler, Director of the Philadelphia VA Medical Center Microbiology laboratory.

For microcolony dispersion assays, microcolonies were grown in Mattek glass bottom dishes inoculated with PAO-GFP in LB + genatmycin, and incubated at 37 °C for 48 hours. Microcolonies (signifying the onset of biofilm formation) were visualized on a confocal microscope at 60×; dispersion was induced by washing out the LB media and replacing it with HBSS plus gentamycin (with glucose as the only nutrient source). Images were taken every 10 min over the course of several hours. Analysis was complicated by the fact that, once cells detached from the coverslip, they became motile and swam in and out of the field of view randomly; for this reason, raw fluorescence intensity or fluorescence area could not be used to quantify the number of cells remaining. A simple image processing workflow was used to measure only those static cells that were in the original first field of view. Image stacks (1 time course of 1 field of view) were first converted to 8 bit, and automatic thresholding was used to create a binary mask (background = 255, cells = 0) of the first image of the stack (time = 0) that was then applied to the entire image stack to minimize the contribution of cells swimming in and out of the image during the time course (i.e. all fluorescence outside of the area of the original non-motile cells was ignored). This allowed measurement of only those cells that were stuck to the coverslip in the first image. To minimize the effects (albeit minimal) of GFP photobleaching over time, the masked image was autothresholded at each timepoint to quanitify the area of signal above background (proportional to the number of cells remaining on the coverslip) rather than the absolute fluorescence.

For determination of salt-sensitivity, wild-type PAO1 *P. aeruginosa* was grown in LB media overnight, followed by resuspension to 0.01 OD in normal saline at the concentrations

indicated. Cells were incubated in low and normal salt solution for 2 hours, followed by dilution and spotting on LB agar plates (incubated overnight at 37°C) to count CFUs. All values were normalized to control (0.9% saline) values obtained within the same experiment (n = 3–4 experiments for each condition).

Human Primary Sinonasal Epithelial Air-Liquid Interface Cell Culture

Primary air-liquid interface (ALI) cultures were set up as previously described (8, 14, 64, 92–94). Tissue was obtained from patients recruited from the Department of Otorhinolaryngology - Head and Neck Surgery Division of Rhinology at the University of Pennsylvania and the Philadelphia Veterans Affairs Medical Center with informed consent and full approval of both Institutional Review Boards. Selection criteria for recruitment were patients undergoing sinonasal surgery. Exclusion criteria included a history of systemic diseases (eg, Wegner's, Sarcoid, Cystic fibrosis, immunodeficiences) and use of antibiotics, oral corticosteroids, or anti-biologics (eg, Xolair) within one month of surgery. Enzymatically dissociated human sinonasal epithelial cells (HSEC) were grown to confluence in DMEM/Ham's F-12 and bronchial epithelial basal medium (BEBM; Clonetics, Cambrex, East Rutherford, NJ) supplemented with 100 U/ml penicillin, 100 μg /ml streptomycin for 7 days. Cells were then trypsinized and seeded on porous polyester membranes in cell culture inserts (Transwell-clear, 12 mm, 0.4 μm pores; Corning, Acton, MA) coated with 100μl of coating solution [BSA (0.1 mg/ml), type I bovine collagen (30 μg/ml), fibronectin (10μg/ml) in LHC basal medium (ThermoFisher)]. Five days later the culture medium was removed from the upper compartment and the epithelium was allowed to differentiate by using differentiation medium consisting of 1:1 DMEM (ThermoFisher) and BEBM (Clonetics) with the Clonetics complements for hEGF (0.5 ng/ml), epinephrine (5 μg/ml), BPE (0.13 mg/ml), hydrocortisone (0.5 μg/ml), insulin (5 μg/ml), triiodothyronine (6.5 μg/ml), and transferrin (0.5 μg/ml), supplemented with 100 UI/ml penicillin, 100 g/ml streptomycin, 0.1 nM retinoic acid, and 10% FBS in the basal compartment.

HEK293T Cell Culture and Transfection

HEK293T cells (ATCC) were cultured in high-glucose DMEM (Gibco) with 10% fetal bovine serum and 1× cell culture penicillin and streptomycin mix. Transfection for heterologous expression experiments was carried out with Lipofectamine 2000 according to the manufacturer's instructions using pcDNA3.1 vectors containing cloned sequences of human *TAS21R2* and *TAS1R3* cDNAs, with N-terminal rat somastostatin receptor 3 and C-terminal HSV tags, as previously described (28). Cells were fixed in 4% paraformaldehyde for 20 min and stained for immunofluorescence at 48 hrs after transfection.

Immunofluroescence Microscopy

Immunofluorescence of fixed HEK293T cells and ALI cultures was carried out as previously described (8, 14). Cells were fixed with 4% paraformaldehyde for 20 min at room temperature, followed by blocking and permeabilization for 1 hour in 0.25% saponin, 1% BSA, 2% normal donkey serum. Antibodies directed against T1R2 and T1R3 were used with Molecular Probes Zenon labeling kit for labeling of rabbit T1R2-directed and rabbit T1R3-directed antibodies. Images were viewed at 20× (HEK293) or 60× (ALIs) on a wide-field inverted microscope (Olympus IX-83, 1.4 N.A. PlanApo objective) running

Metamorph (Molecular Devices, Sunnyvale, CA). After primary antibody incubation overnight at 4°C, secondary antibody incubation was for 2 hrs at 4 °C using Molecular probes AlexaFluor 488-conjugated donkey secondary antibody to detect β-tubulin IV. For HEK293T cell immunofluorescence, T1R2 and/or T1R3 rabbit polyclonal antibodies were used with mouse monoclonal FLAG-tag-directed antibody M2 (Sigma Aldrich) or anti-HA (16B12, ab130275). Donkey secondary antibodies directed against rabbit or mouse IgG and conjugated to AlexaFluor 488 or 555 were used to visualize primary antibody staining. Images were analyzed using Metamorph, Fluoview software, and/or the FIJI (95) version of ImageJ (W. Rasband, Research Services Branch, National Institute of Mental Health, Bethesda, MD).

Live-Cell Imaging of Sinonasal ALI Cultures

Fluo-4 loading and imaging were done exactly as previously described (8, 14, 92). Cells were loaded with 10 μM fluo-4-AM (PBS + 0.1% pluronic F127; apical side only) for ~120 min at room temperature, followed by 3 washes with DPBS and 15–20 min incubation to allow cells to recover. Images were captured at 3 or 5 sec intervals using the 488 nM laser line of an Olympus Fluoview confocal system attached to an Olympus IX81 microscope (10×, 0.3 NA UPlanFLN objective; Olympus). No gain, offset or gamma alterations were used. Normalization of Fluo-4 fluorescence changes was made after subtraction of background, approximated for each experiment by measuring unloaded ALIs. Baseline fluorescence (F_o) was determined by averaging the first 10 frames of each experiment.

Live/Dead staining of ALIs was performed using Syto9/PI mix of a *Bac*Light® live/dead kit. MRSA-M2 overnight cultures were centrifuged, normalized to OD 0.01, and incubated with human ALI cultures for 6 hours at 37° C. Afterward, ALIs were washed copiously with PBS and stained using the two dyes at concentrations indicated in the manufacturers instructions and imaged immediately.

Data Analyses and Statistics

All statistical analyses were performed in GraphPad Prism; $P < 0.05$ was considered statistically significant. For multiple comparisons, ANOVA with Bonferroni post-test was used when pre-selected pairwise comparisons were performed, ANOVA with Tukey-Kramer post-test was used when all values in the data set were compared, and ANOVA with Dunnett post-test was used when all values were compared with a control value. Tests used are indicated in the figure legend. For all figures, * = $P < 0.05$, ** = $P < 0.01$, and *n.s.* = no statistical significance.

Supplementary Material

Refer to Web version on PubMed Central for supplementary material.

Acknowledgments

The authors thank Dr. L. Chandler and the Philadelphia Veterans Affairs Medical Center microbiology lab for help with speciation of clinically isolated sinonasal bacterial cultures and antibiotic resistance testing, as well as Dr. I. Nissim and the Children's Hospital of Philadelphia Metabolomics Core for LC-MS/MS identification of D-amino

acids produced by bacteria. The authors thank Dr. A. Mitchell of Carnegie Mellon University for initially pointing out to the authors that bacteria produce D-amino acids.

Funding: This work was supported by NIH grants R01DC013588 (to N.A.C.), R21DC013886 (to N.A.C.) and R03DC013862 (to R.J.L.), Cystic Fibrosis Foundation grant LEER16G0 to R.J.L., a pilot grant from the University of Pennsylvania Diabetes Research Center (supported through NIH grant DK19525) to R.J.L., and a philanthropic donation from the R.L.G. Foundation, Inc to N.A.C.

References

1. Hariri BM, Cohen NA. New insights into upper airway innate immunity. Am J Rhinol Allergy. 2016; 30:319–323. [PubMed: 27657896]
2. Kennedy JL, Borish L. Chronic rhinosinusitis and antibiotics: the good, the bad, and the ugly. Am J Rhinol Allergy. 2013; 27:467–472. [PubMed: 24274221]
3. Settipane RA, Peters AT, Chandra R. Chapter 4: Chronic rhinosinusitis. Am J Rhinol Allergy. 2013; 27(Suppl 1):S11–15. [PubMed: 23711032]
4. Fokkens WJ, Lund VJ, Mullol J, Bachert C, Alobid I, Baroody F, Cohen N, Cervin A, Douglas R, Gevaert P, Georgalas C, Goossens H, Harvey R, Hellings P, Hopkins C, Jones N, Joos G, Kalogjera L, Kern B, Kowalski M, Price D, Riechelmann H, Schlosser R, Senior B, Thomas M, Toskala E, Voegels R, Wang de Y, Wormald PJ. European Position Paper on Rhinosinusitis and Nasal Polyps 2012. Rhinol Suppl. 2012; 3:1–298. p preceding table of contents.
5. Marcinkiewicz J, Strus M, Pasich E. Antibiotic resistance: a “dark side” of biofilmassociated chronic infections. Pol Arch Med Wewn. 2013; 123:309–313. [PubMed: 23828150]
6. Rujanavej V, Soudry E, Banaei N, Baron EJ, Hwang PH, Nayak JV. Trends in incidence and susceptibility among methicillin-resistant Staphylococcus aureus isolated from intranasal cultures associated with rhinosinusitis. Am J Rhinol Allergy. 2013; 27:134–137. [PubMed: 23562203]
7. Manes RP, Batra PS. Bacteriology and antibiotic resistance in chronic rhinosinusitis. Facial Plast Surg Clin North Am. 2012; 20:87–91. [PubMed: 22099621]
8. Lee RJ, Kofonow JM, Rosen PL, Siebert AP, Chen B, Doghramji L, Xiong G, Adappa ND, Palmer JN, Kennedy DW, Kreindler JL, Margolskee RF, Cohen NA. Bitter and sweet taste receptors regulate human upper respiratory innate immunity. J Clin Invest. 2014; 124:1393–1405. [PubMed: 24531552]
9. Margolskee RF. Teaching resources. Sensory systems: taste perception. Sci STKE. 2005; 2005:tr20.
10. Margolskee RF. The molecular biology of taste transduction. Bioessays. 1993; 15:645–650. [PubMed: 7506022]
11. Laffitte A, Neiers F, Briand L. Functional roles of the sweet taste receptor in oral and extraoral tissues. Curr Opin Clin Nutr Metab Care. 2014
12. Depoortere I. Taste receptors of the gut: emerging roles in health and disease. Gut. 2014; 63:179–190. [PubMed: 24131638]
13. Lee RJ, Cohen NA. Taste receptors in innate immunity. Cell Mol Life Sci. 2015; 72:217–236. [PubMed: 25323130]
14. Lee RJ, Xiong G, Kofonow JM, Chen B, Lysenko A, Jiang P, Abraham V, Doghramji L, Adappa ND, Palmer JN, Kennedy DW, Beauchamp GK, Doulias PT, Ischiropoulos H, Kreindler JL, Reed DR, Cohen NA. T2R38 taste receptor polymorphisms underlie susceptibility to upper respiratory infection. J Clin Invest. 2012; 122:4145–4159. [PubMed: 23041624]
15. Deckmann K, Filipski K, Krasteva-Christ G, Fronius M, Althaus M, Rafiq A, Papadakis T, Renno L, Jurastow I, Wessels L, Wolff M, Schutz B, Weihe E, Chubanov V, Gudermann T, Klein J, Bschleipfer T, Kummer W. Bitter triggers acetylcholine release from polymodal urethral chemosensory cells and bladder reflexes. Proc Natl Acad Sci U S A. 2014; 111:8287–8292. [PubMed: 24843119]
16. Maurer S, Wabnitz GH, Kahle NA, Stegmaier S, Prior B, Giese T, Gaida MM, Samstag Y, Hansch GM. Tasting Pseudomonas aeruginosa Biofilms: Human Neutrophils Express the Bitter Receptor T2R38 as Sensor for the Quorum Sensing Molecule N-(3-Oxododecanoyl)-l-Homoserine Lactone. Front Immunol. 2015; 6:369. [PubMed: 26257736]

17. Tizzano M, Gulbransen BD, Vandenbeuch A, Clapp TR, Herman JP, Sibhatu HM, Churchill ME, Silver WL, Kinnamon SC, Finger TE. Nasal chemosensory cells use bitter taste signaling to detect irritants and bacterial signals. Proc Natl Acad Sci U S A. 2010; 107:3210–3215. [PubMed: 20133764]
18. Saunders CJ, Christensen M, Finger TE, Tizzano M. Cholinergic neurotransmission links solitary chemosensory cells to nasal inflammation. Proc Natl Acad Sci U S A. 2014; 111:6075–6080. [PubMed: 24711432]
19. Finger TE. Evolution of taste and solitary chemoreceptor cell systems. Brain Behav Evol. 1997; 50:234–243. [PubMed: 9310198]
20. Hansen A. Olfactory and solitary chemosensory cells: two different chemosensory systems in the nasal cavity of the American alligator, Alligator mississippiensis. BMC Neurosci. 2007; 8:64. [PubMed: 17683564]
21. Tizzano M, Cristofoletti M, Sbarbati A, Finger TE. Expression of taste receptors in solitary chemosensory cells of rodent airways. BMC Pulm Med. 2011; 11:3. [PubMed: 21232137]
22. Gulbransen BD, Clapp TR, Finger TE, Kinnamon SC. Nasal solitary chemoreceptor cell responses to bitter and trigeminal stimulants in vitro. J Neurophysiol. 2008; 99:2929–2937. [PubMed: 18417634]
23. Finger TE, Bottger B, Hansen A, Anderson KT, Alimohammadi H, Silver WL. Solitary chemoreceptor cells in the nasal cavity serve as sentinels of respiration. Proc Natl Acad Sci U S A. 2003; 100:8981–8986. [PubMed: 12857948]
24. Barham HP, Cooper SE, Anderson CB, Tizzano M, Kingdom TT, Finger TE, Kinnamon SC, Ramakrishnan VR. Solitary chemosensory cells and bitter taste receptor signaling in human sinonasal mucosa. Int Forum Allergy Rhinol. 2013; 3:450–457. [PubMed: 23404938]
25. Margolskee RF. Molecular mechanisms of bitter and sweet taste transduction. J Biol Chem. 2002; 277:1–4. [PubMed: 11696554]
26. Cui M, Jiang P, Maillet E, Max M, Margolskee RF, Osman R. The heterodimeric sweet taste receptor has multiple potential ligand binding sites. Curr Pharm Des. 2006; 12:4591–4600. [PubMed: 17168764]
27. Jiang P, Cui M, Zhao B, Liu Z, Snyder LA, Benard LM, Osman R, Margolskee RF, Max M. Lactisole interacts with the transmembrane domains of human T1R3 to inhibit sweet taste. J Biol Chem. 2005; 280:15238–15246. [PubMed: 15668251]
28. Jiang P, Cui M, Zhao B, Snyder LA, Benard LM, Osman R, Max M, Margolskee RF. Identification of the cyclamate interaction site within the transmembrane domain of the human sweet taste receptor subunit T1R3. J Biol Chem. 2005; 280:34296–34305. [PubMed: 16076846]
29. Imada T, Misaka T, Fujiwara S, Okada S, Fukuda Y, Abe K. Amiloride reduces the sweet taste intensity by inhibiting the human sweet taste receptor. Biochem Biophys Res Commun. 2010; 397:220–225. [PubMed: 20493823]
30. Garnett JP, Baker EH, Baines DL. Sweet talk: insights into the nature and importance of glucose transport in lung epithelium. Eur Respir J. 2012; 40:1269–1276. [PubMed: 22878875]
31. Kalsi KK, Baker EH, Fraser O, Chung YL, Mace OJ, Tarelli E, Philips BJ, Baines DL. Glucose homeostasis across human airway epithelial cell monolayers: role of diffusion, transport and metabolism. Pflugers Arch. 2009; 457:1061–1070. [PubMed: 18781323]
32. Pezzulo AA, Gutierrez J, Duschner KS, McConnell KS, Taft PJ, Ernst SE, Yahr TL, Rahmouni K, Klesney-Tait J, Stoltz DA, Zabner J. Glucose depletion in the airway surface liquid is essential for sterility of the airways. PLoS One. 2011; 6:e16166. [PubMed: 21311590]
33. Bassoli A, Borgonovo G, Caremoli F, Mancuso G. The taste of D- and L-amino acids: In vitro binding assays with cloned human bitter (TAS2Rs) and sweet (TAS1R2/TAS1R3) receptors. Food Chem. 2014; 150:27–33. [PubMed: 24360415]
34. Zhang G, Sun HJ. Racemization in reverse: evidence that D-amino acid toxicity on Earth is controlled by bacteria with racemases. PLoS One. 2014; 9:e92101. [PubMed: 24647559]
35. Lam H, Oh DC, Cava F, Takacs CN, Clardy J, de Pedro MA, Waldor MK. D-amino acids govern stationary phase cell wall remodeling in bacteria. Science. 2009; 325:1552–1555. [PubMed: 19762646]

36. Kolodkin-Gal I, Romero D, Cao S, Clardy J, Kolter R, Losick R. D-amino acids trigger biofilm disassembly. Science. 2010; 328:627–629. [PubMed: 20431016]
37. Brandenburg KS, Rodriguez KJ, McAnulty JF, Murphy CJ, Abbott NL, Schurr MJ, Czuprynski CJ. Tryptophan inhibits biofilm formation by Pseudomonas aeruginosa. Antimicrob Agents Chemother. 2013; 57:1921–1925. [PubMed: 23318791]
38. Yu C, Wu J, Contreras AE, Li Q. Control of nanofiltration membrane biofouling by Pseudomonas aeruginosa using d-tyrosine. J Membrane Sci. 2012; 423–424:487–494.
39. Harmata AJ, Ma Y, Sanchez CJ, Zienkiewicz KJ, Elefteriou F, Wenke JC, Guelcher SA. D-amino acid inhibits biofilm but not new bone formation in an ovine model. Clin Orthop Relat Res. 2015; 473:3951–3961. [PubMed: 26201421]
40. Hochbaum AI, Kolodkin-Gal I, Foulston L, Kolter R, Aizenberg J, Losick R. Inhibitory effects of D-amino acids on Staphylococcus aureus biofilm development. J Bacteriol. 2011; 193:5616–5622. [PubMed: 21856845]
41. Ramon-Perez ML, Diaz-Cedillo F, Ibarra JA, Torales-Cardena A, Rodriguez-Martinez S, Jan-Roblero J, Cancino-Diaz ME, Cancino-Diaz JC. D-Amino acids inhibit biofilm formation in Staphylococcus epidermidis strains from ocular infections. J Med Microbiol. 2014; 63:1369–1376. [PubMed: 25001104]
42. Sanchez CJ Jr, Akers KS, Romano DR, Woodbury RL, Hardy SK, Murray CK, Wenke JC. D-amino acids enhance the activity of antimicrobials against biofilms of clinical wound isolates of Staphylococcus aureus and Pseudomonas aeruginosa. Antimicrob Agents Chemother. 2014; 58:4353–4361. [PubMed: 24841260]
43. Xu H, Liu Y. d-Amino acid mitigated membrane biofouling and promoted biofilm detachment. J Membrane Sci. 2011; 376:266–275.
44. Xua H, Liu Y. Reduced microbial attachment by d-amino acid-inhibited AI-2 and EPS production. Water Res. 2011; 45:5796–5804. [PubMed: 21924452]
45. Xing SF, Sun XF, Taylor AA, Walker SL, Wang YF, Wang SG. D-amino acids inhibit initial bacterial adhesion: thermodynamic evidence. Biotechnol Bioeng. 2015; 112:696–704. [PubMed: 25333717]
46. Yang J, Yu J, Jiang J, Liang C, Feng Y. D-tyrosine affects aggregation behavior of Pantoea agglomerans. J Basic Microbiol. 2016
47. Sarkar S, Pires MM. d-Amino acids do not inhibit biofilm formation in Staphylococcus aureus. PLoS One. 2015; 10:e0117613. [PubMed: 25658642]
48. Leiman SA, May JM, Lebar MD, Kahne D, Kolter R, Losick R. D-amino acids indirectly inhibit biofilm formation in Bacillus subtilis by interfering with protein synthesis. J Bacteriol. 2013; 195:5391–5395. [PubMed: 24097941]
49. Li Y, Jia R, Al-Mahamedh HH, Xu D, Gu T. Enhanced Biocide Mitigation of Field Biofilm Consortia by a Mixture of D-Amino Acids. Front Microbiol. 2016; 7:896. [PubMed: 27379039]
50. She P, Chen L, Liu H, Zou Y, Luo Z, Koronfel A, Wu Y. The effects of D-Tyrosine combined with amikacin on the biofilms of Pseudomonas aeruginosa. Microb Pathog. 2015; 86:38–44. [PubMed: 26188263]
51. Yu C, Li X, Zhang N, Wen D, Liu C, Li Q. Inhibition of biofilm formation by D-tyrosine: Effect of bacterial type and D-tyrosine concentration. Water Res. 2016; 92:173–179. [PubMed: 26854605]
52. Cava F, Lam H, de Pedro MA, Waldor MK. Emerging knowledge of regulatory roles of D-amino acids in bacteria. Cell Mol Life Sci. 2011; 68:817–831. [PubMed: 21161322]
53. Shallenberger RS, Acree TE, Lee CY. Sweet taste of D and L-sugars and amino-acids and the steric nature of their chemo-receptor site. Nature. 1969; 221:555–556. [PubMed: 5794306]
54. Bjarnadottir TK, Fredriksson R, Schioth HB. The gene repertoire and the common evolutionary history of glutamate, pheromone (V2R), taste(1) and other related G protein-coupled receptors. Gene. 2005; 362:70–84. [PubMed: 16229975]
55. Nuemket N, Yasui N, Kusakabe Y, Nomura Y, Atsumi N, Akiyama S, Nango E, Kato Y, Kaneko MK, Takagi J, Hosotani M, Yamashita A. Structural basis for perception of diverse chemical substances by T1r taste receptors. Nat Commun. 2017; 8:15530. [PubMed: 28534491]
56. Morris JA, Martenson R, Deibler G, Cagan RH. Characterization of monellin, a protein that tastes sweet. J Biol Chem. 1973; 248:534–539. [PubMed: 4684691]

57. Tizzano M, Finger TE. Chemosensors in the nose: guardians of the airways. Physiology (Bethesda). 2013; 28:51–60. [PubMed: 23280357]
58. Lee RJ, Cohen NA. Sinonasal solitary chemosensory cells “taste” the upper respiratory environment to regulate innate immunity. Am J Rhinol Allergy. 2014; 28:366–373. [PubMed: 25198020]
59. Schiffman SS, Sennewald K, Gagnon J. Comparison of taste qualities and thresholds of D- and L-amino acids. Physiol Behav. 1981; 27:51–59. [PubMed: 7267802]
60. Solms J, Vuataz L, Egli RH. The taste of L- and D-amino acids. Experientia. 1965; 21:692–694. [PubMed: 5869699]
61. Kawai M, Sekine-Hayakawa Y, Okiyama A, Ninomiya Y. Gustatory sensation of (L)- and (D)-amino acids in humans. Amino Acids. 2012; 43:2349–2358. [PubMed: 22588481]
62. Ha DG, Kuchma SL, O’Toole GA. Plate-based assay for swarming motility in Pseudomonas aeruginosa. Methods Mol Biol. 2014; 1149:67–72. [PubMed: 24818898]
63. Caiazza NC, Shanks RM, O’Toole GA. Rhamnolipids modulate swarming motility patterns of Pseudomonas aeruginosa. J Bacteriol. 2005; 187:7351–7361. [PubMed: 16237018]
64. Lai Y, Chen B, Shi J, Palmer JN, Kennedy DW, Cohen NA. Inflammation-mediated upregulation of centrosomal protein 110, a negative modulator of ciliogenesis, in patients with chronic rhinosinusitis. J Allergy Clin Immunol. 2011; 128:1207–1215. e1201. [PubMed: 21982113]
65. Lee RJ, Cohen NA. Bitter and sweet taste receptors in the respiratory epithelium in health and disease. J Mol Med (Berl). 2014; 92:1235–1244. [PubMed: 25391251]
66. Dimova S, Brewster ME, Noppe M, Jorissen M, Augustijns P. The use of human nasal in vitro cell systems during drug discovery and development. Toxicol In Vitro. 2005; 19:107–122. [PubMed: 15582362]
67. Sanematsu K, Kusakabe Y, Shigemura N, Hirokawa T, Nakamura S, Imoto T, Ninomiya Y. Molecular Mechanisms for Sweet-suppressing Effect of Gymnemic Acids. J Biol Chem. 2014; 289:25711–25720. [PubMed: 25056955]
68. Meiselman HL, Halpern BP. Effects of Gymnema sylvestre on complex tastes elicited by amino acids and sucrose. Physiol Behav. 1970; 5:1379–1384. [PubMed: 5524525]
69. Gill SK, Hui K, Farne H, Garnett JP, Baines DL, Moore LS, Holmes AH, Filloux A, Tregoning JS. Increased airway glucose increases airway bacterial load in hyperglycaemia. Sci Rep. 2016; 6:27636. [PubMed: 27273266]
70. Garnett JP, Nguyen TT, Moffatt JD, Pelham ER, Kalsi KK, Baker EH, Baines DL. Proinflammatory mediators disrupt glucose homeostasis in airway surface liquid. J Immunol. 2012; 189:373–380. [PubMed: 22623330]
71. Baker EH, Clark N, Brennan AL, Fisher DA, Gyi KM, Hodson ME, Philips BJ, Baines DL, Wood DM. Hyperglycemia and cystic fibrosis alter respiratory fluid glucose concentrations estimated by breath condensate analysis. J Appl Physiol (1985). 2007; 102:1969–1975. [PubMed: 17303703]
72. Rasmussen TT, Kirkeby LP, Poulsen K, Reinholdt J, Kilian M. Resident aerobic microbiota of the adult human nasal cavity. APMIS. 2000; 108:663–675. [PubMed: 11200821]
73. Hamilos DL. Host-microbial interactions in patients with chronic rhinosinusitis. J Allergy Clin Immunol. 2014; 133:640–653. e644. [PubMed: 24290275]
74. Sivaraman K, Venkataraman N, Cole AM. Staphylococcus aureus nasal carriage and its contributing factors. Future Microbiol. 2009; 4:999–1008. [PubMed: 19824791]
75. Verhoeven PO, Gagnaire J, Botelho-Nevers E, Grattard F, Carricajo A, Lucht F, Pozzetto B, Berthelot P. Detection and clinical relevance of Staphylococcus aureus nasal carriage: an update. Expert Rev Anti Infect Ther. 2014; 12:75–89. [PubMed: 24308709]
76. Krismer B, Peschel A. Does Staphylococcus aureus nasal colonization involve biofilm formation? Future Microbiol. 2011; 6:489–493. [PubMed: 21585258]
77. Muir A, Soong G, Sokol S, Reddy B, Gomez MI, Van Heeckeren A, Prince A. Toll-like receptors in normal and cystic fibrosis airway epithelial cells. Am J Respir Cell Mol Biol. 2004; 30:777–783. [PubMed: 14656745]
78. Mfuna Endam L, Filali-Mouhim A, Boisvert P, Boulet LP, Bosse Y, Desrosiers M. Genetic variations in taste receptors are associated with chronic rhinosinusitis: a replication study. Int Forum Allergy Rhinol. 2014; 4:200–206. [PubMed: 24415641]

79. Meyer-Gerspach AC, Wolnerhanssen B, Beglinger C. Gut sweet taste receptors and their role in metabolism. Front Horm Res. 2014; 42:123–133. [PubMed: 24732930]
80. Elliott RA, Kapoor S, Tincello DG. Expression and distribution of the sweet taste receptor isoforms T1R2 and T1R3 in human and rat bladders. J Urol. 2011; 186:2455–2462. [PubMed: 22019168]
81. Jones DT, Taylor WR, Thornton JM. The rapid generation of mutation data matrices from protein sequences. Comput Appl Biosci. 1992; 8:275–282. [PubMed: 1633570]
82. Tamura K, Stecher G, Peterson D, Filipski A, Kumar S. MEGA6: Molecular Evolutionary Genetics Analysis version 6.0. Mol Biol Evol. 2013; 30:2725–2729. [PubMed: 24132122]
83. Shirtliff ME, Calhoun JH, Mader JT. Experimental osteomyelitis treatment with antibiotic-impregnated hydroxyapatite. Clin Orthop Relat Res. 2002:239–247.
84. Pearson JP, Gray KM, Passador L, Tucker KD, Eberhard A, Iglewski BH, Greenberg EP. Structure of the autoinducer required for expression of Pseudomonas aeruginosa virulence genes. Proc Natl Acad Sci U S A. 1994; 91:197–201. [PubMed: 8278364]
85. Pearson JP, Pesci EC, Iglewski BH. Roles of Pseudomonas aeruginosa las and rhl quorum-sensing systems in control of elastase and rhamnolipid biosynthesis genes. J Bacteriol. 1997; 179:5756–5767. [PubMed: 9294432]
86. O'Toole GA. Microtiter dish biofilm formation assay. J Vis Exp. 2011
87. Essar DW, Eberly L, Hadero A, Crawford IP. Identification and characterization of genes for a second anthranilate synthase in Pseudomonas aeruginosa: interchangeability of the two anthranilate synthases and evolutionary implications. J Bacteriol. 1990; 172:884–900. [PubMed: 2153661]
88. Lundgren BR, Thornton W, Dornan MH, Villegas-Penaranda LR, Boddy CN, Nomura CT. Gene PA2449 is essential for glycine metabolism and pyocyanin biosynthesis in Pseudomonas aeruginosa PAO1. J Bacteriol. 2013; 195:2087–2100. [PubMed: 23457254]
89. Ha DG, Kuchma SL, O'Toole GA. Plate-based assay for swimming motility in Pseudomonas aeruginosa. Methods Mol Biol. 2014; 1149:59–65. [PubMed: 24818897]
90. Hariri BM, Payne SJ, Chen B, Mansfield C, Doghramji LJ, Adappa ND, Palmer JN, Kennedy DW, Niv MY, Lee RJ. In vitro effects of anthocyanidins on sinonasal epithelial nitric oxide production and bacterial physiology. Am J Rhinol Allergy. 2016; 30:261–268. [PubMed: 27456596]
91. Hindler, J. Clinical Microbiology Procedures Handbook. 2. Isenberg, HD., editor. Vol. chap. 5. ASM Press; Washington, D.C: 2005.
92. Lee RJ, Chen B, Doghramji L, Adappa ND, Palmer JN, Kennedy DW, Cohen NA. Vasoactive intestinal peptide regulates sinonasal mucociliary clearance and synergizes with histamine in stimulating sinonasal fluid secretion. FASEB J. 2013; 27:5094–5103. [PubMed: 23934280]
93. Zhao KQ, Cowan AT, Lee RJ, Goldstein N, Droguett K, Chen B, Zheng C, Villalon M, Palmer JN, Kreindler JL, Cohen NA. Molecular modulation of airway epithelial ciliary response to sneezing. FASEB J. 2012; 26:3178–3187. [PubMed: 22516297]
94. Hariri BM, McMahon DB, Chen B, Freund JR, Mansfield CJ, Doghramji LJ, Adappa ND, Palmer JN, Kennedy DW, Reed DR, Jiang P, Lee RJ. Flavones modulate respiratory epithelial innate immunity: anti-inflammatory effects and activation of the T2R14 receptor. J Biol Chem. 2017; 292:8484–8497. [PubMed: 28373278]
95. Schindelin J, Arganda-Carreras I, Frise E, Kaynig V, Longair M, Pietzsch T, Preibisch S, Rueden C, Saalfeld S, Schmid B, Tinevez JY, White DJ, Hartenstein V, Eliceiri K, Tomancak P, Cardona A. Fiji: an open-source platform for biological-image analysis. Nat Methods. 2012; 9:676–682. [PubMed: 22743772]

Editor's Summary

Stimulation of the sweet taste receptor (T1R2/3) in solitary chemosensory cells (SCCs) of the upper respiratory epithelium inhibits the release of antimicrobial peptides by neighboring epithelial cells. In addition to being activated by various sugars, T1R can also be activated by some D-amino acids. Lee *et al.* found that *Staphylococcus* species present in the nasal cavity of chronic rhinosinusitis patients produced D-Phe and D-Leu, both of which can activate T1R2/3. Treatment of primary human sinonasal epithelial cultures with D-Phe and D-Leu inhibited the release of antimicrobial peptides and increased cell death in response to infection with methicillin-resistant *S. aureus*. D-Phe and D-Leu, as well as conditioned medium from respiratory isolates of *Staphylococcus*, inhibited the formation of *Pseudomonas aaeruginosa* biofilms. These findings demonstrate that D-amino acids produced by nasal flora can inhibit innate immune responses through T1R2/3 and may play a role in shaping the microbial community of the airways.

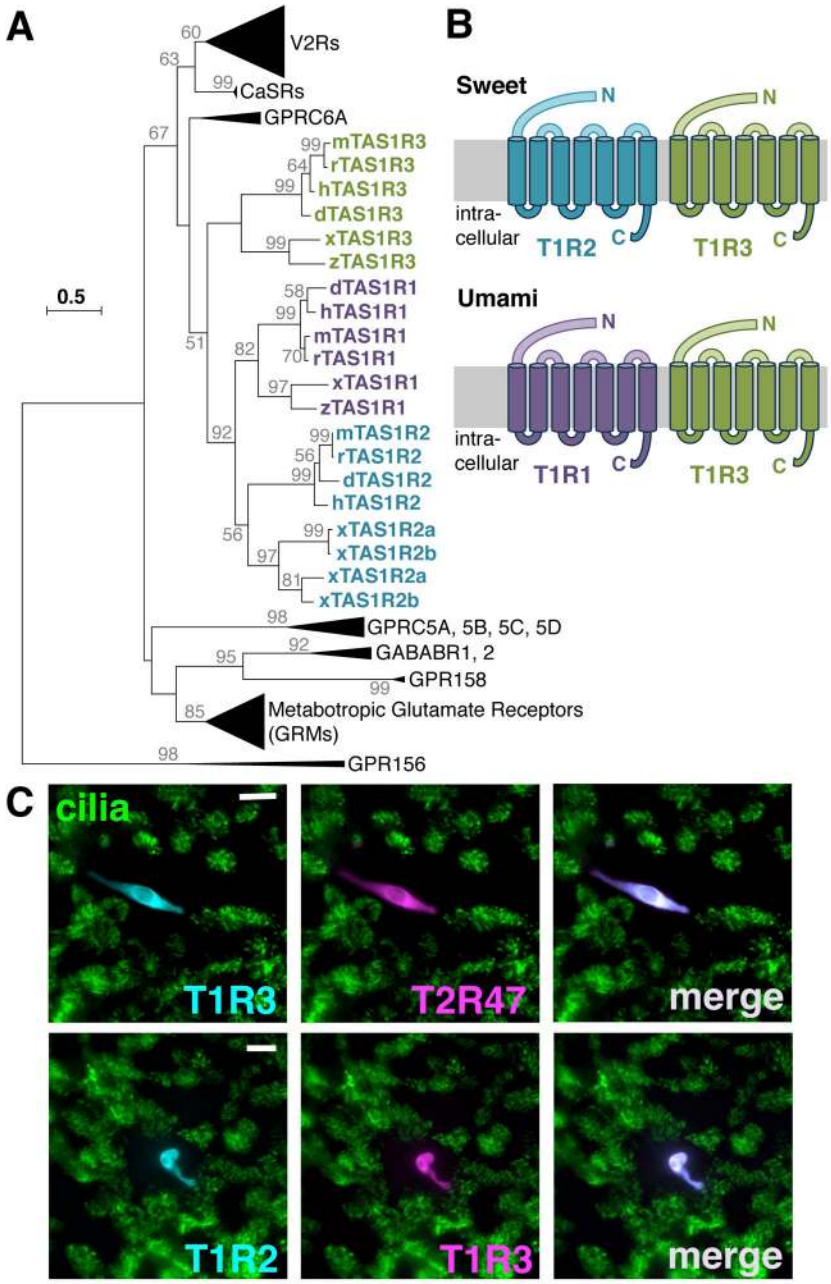

Fig. 1. Evolutionary relationship of sweet and umami taste receptor subunits

(A) Condensed evolutionary tree showing mouse (m), rat (r), human (h), dog (d), frog (x), and zebrafish (z) Tas1R1 (purple), Tas1R2 (blue), and Tas1R3 (green) subunits within the class C G protein–coupled receptor family. This family also includes the V2R pheromone receptors, the calcium-sensing receptors (CaSRs), the metabotropic glutamate receptors, and the other GPCRs indicated in black text. The full tree is shown in fig. S1. **(B)** Tas1R3 (T1R3) combines with Tas1R2 (T1R2) or Tas1R1 (T1R1) to form the sweet or umami receptors, respectively. **(C)** Sinonasal solitary chemosensory cells in human primary sinonasal air-liquid interface (ALI) cultures produce both T1R2 and T1R3 sweet taste

receptor subunits. Images are representative of 3 independent experiments using ALIs from 3 individual patients. Scale bars, 20 μm.

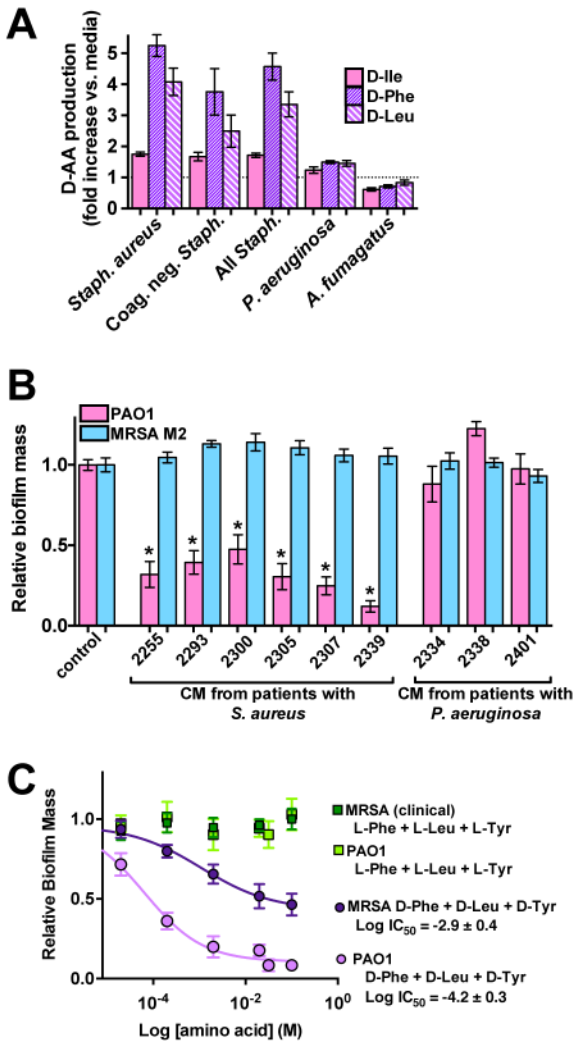

Fig. 2. Bacteria and sweet D-amino acids in clinical sinonasal microbiologic cultures and effects on biofilm formation

(A) Fold increases in D-Phe, D-Leu, and D-Ile from sinonasal microorganism-conditioned medium (CM) compared to starting medium. N = 5–12 independent culture samples for each condition tested separately for each D-amino acid. **(B)** Biofilm formation by *P. aeruginosa* strain PAO-1 and methicillin-resistant *S. aureus* (MRSA) strain M2 in the presence of CM from the indicated patient samples. N = 6–10 independent experiments for each condition and concentration; each single experiment represents an average of >8 wells of a 96 well plate. * p <0.05 by 1-way ANOVA, Dunnett's post test comparing values to strain-specific control. **(C)** Dose-dependent effects of L-Phe + L-Leu + L-Tyr or D-Phe + D-Leu + D-Tyr on *P. aeruginosa* PAO-1 and MRSA biofilm formation. Due to the poor solubility of L-Tyr and D-Tyr, the maximum concentration of L-Tyr or D-Tyr in these experiments was 0.1 mM. For amino acid concentrations indicated as greater than 0.1mM on the graph, the indicated concentration refers to the concentration of L-Phe or D-Phe and L-Leu or D-Leu, with L-Tyr or D-Tyr at 0.1 mM. N = 6–10 independent experiments for each condition and concentration; each single experiment represents an average of >8-wells of a 96 well plate.

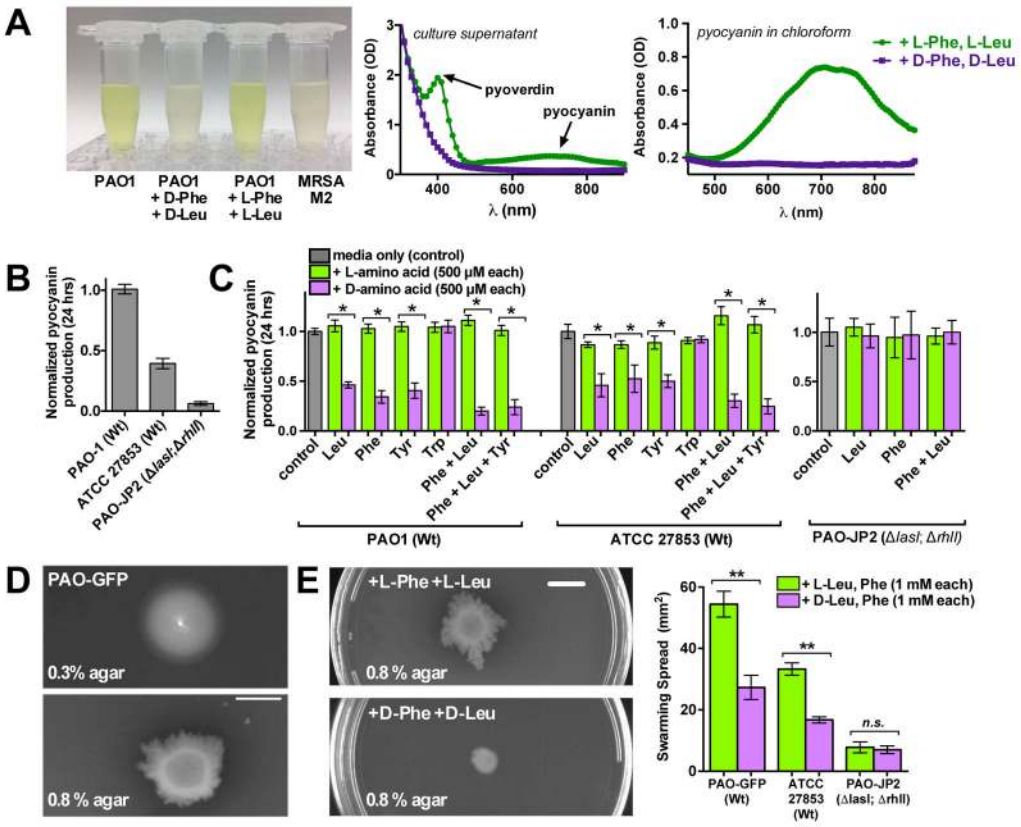

Fig. 3. Effects of sweet D-amino acids on *P. aeruginosa* pyocyanin production and swarming

(A) Color of PAO-1 supernatant in the presence of L- or D-amino acids and representative absorption spectra of supernatant or chloroform-extracted pyocyanin. N = 3–10 independent experiments per strain per condition; each experiment averaged 3 suspension cultures. **(B)** Bar graph of relative pyocyanin abundance in *P. aeruginosa* strains. N = 3 independent experiments for each strain; each single experiment averaged 3 suspension cultures. **(C)** Quantification of relative pyocyanin abundance in strains PAO1 and ATCC27853, which are biofilm-competent, and PAO-JP2, which cannot form biofilms. N = 3–10 independent experiments per strain per condition; each single experiment averaged 3 suspension cultures. **(D)** Morphology of PAO-GFP colonies under conditions that favor swimming (0.3% agar) or swarming (0.8% agar). Scale bar, 1cm. **(E)** Morphology of PAO-GFP colonies under swarming conditions and quantification of swarming in the presence of D-Phe and D-Leu. Scale bar, 1cm. Graphs show mean ± SEM with * = p <0.05 and ** p <0.01 (1-way ANOVA, Bonferronni post test comparing bracketed groups). N = 5 independent experiments for each condition per strain; each experiment averaged 3 plates.

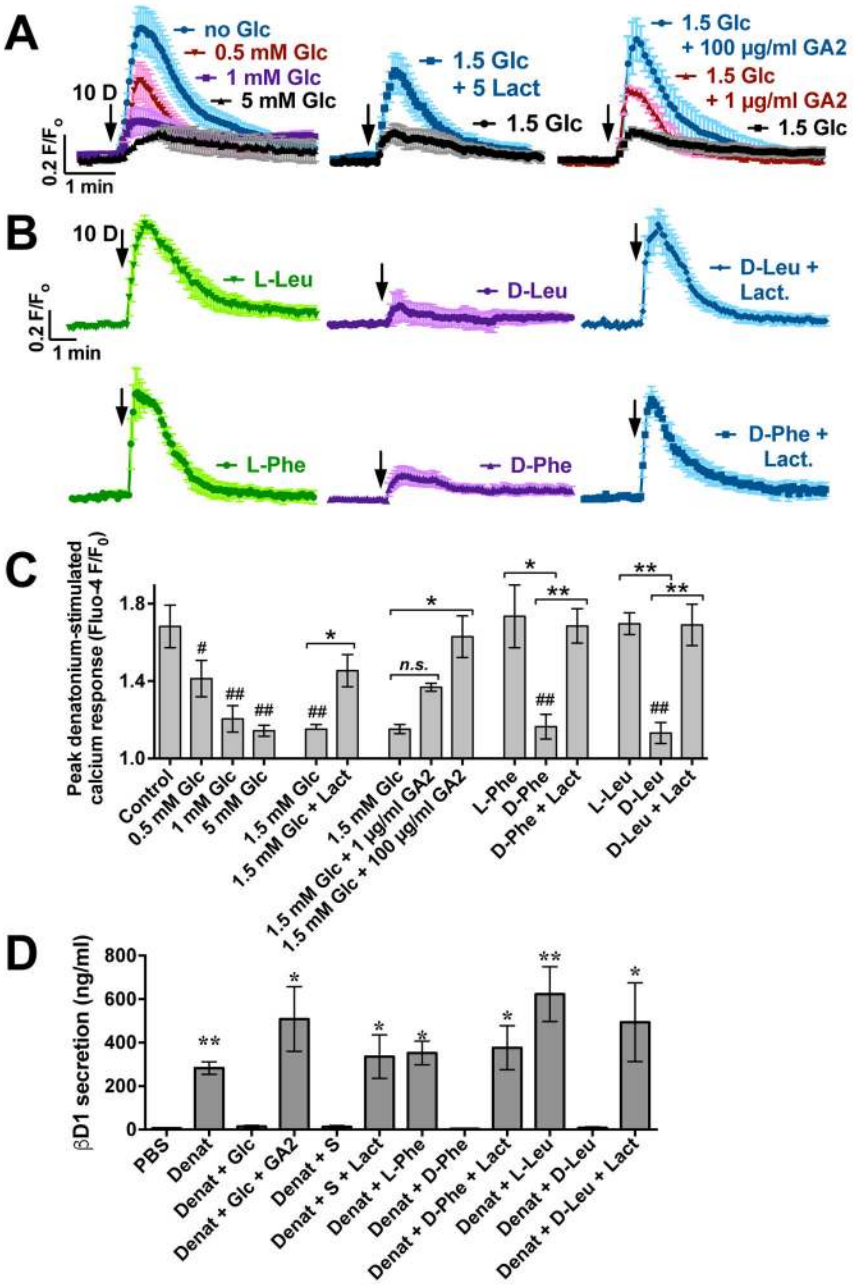

Fig. 4. Effects of D-amino acids on SCC T2R Ca^{2+} responses

(A) Ca^{2+} responses of SCCs treated with denatonium (10 mM applied apically; abbreviated 10D) in the presence or absence of glucose (Glc) ± lactisole (Lact)or gymnemic acid 2 (GA2). Traces shown are the average (± SEM) of multiple experiments (N = 6–10); each experiment was performed on a single air-liquid interface (ALI) culture from a separate individual patients (thus cells from 6–10 patients were examined per condition) **(B)** Calcium responses in the presence of D-Leu or L-Leu (2 mM; top) and D-Phe or L-Phe (2 mM; bottom) ± lactisole. N = 5–8 experiments, each experiment was performed on a single ALI from a separate individual patient (thus cells from 5–8 patients were examined per

condition). **(C)** Summary of peak fluo-4 F/F_o values for data shown in panels A and B. Pound symbols (#) indicate significance compared with control (denatonium only); asterisks denote significance between brackets; # and * = p <0.05 and ## and ** = p <0.01 by one-way ANOVA with Bonferroni post-test. **(D)** β-defensin secreted into airway surface liquid (ASL) after treatment with the indicated combinations of denatonium (Denat), glucose (Glc), gymnemic acis (GA2), sucralose (S), and lactisole (Lact) in PBS. N = 4–6 ALI cultures per condition, each from a separate individual patient; * = p <0.05 and ** = p <0.01 compared with PBS (unstimulated control) by one-way ANOVA with Dunnett's post-test.

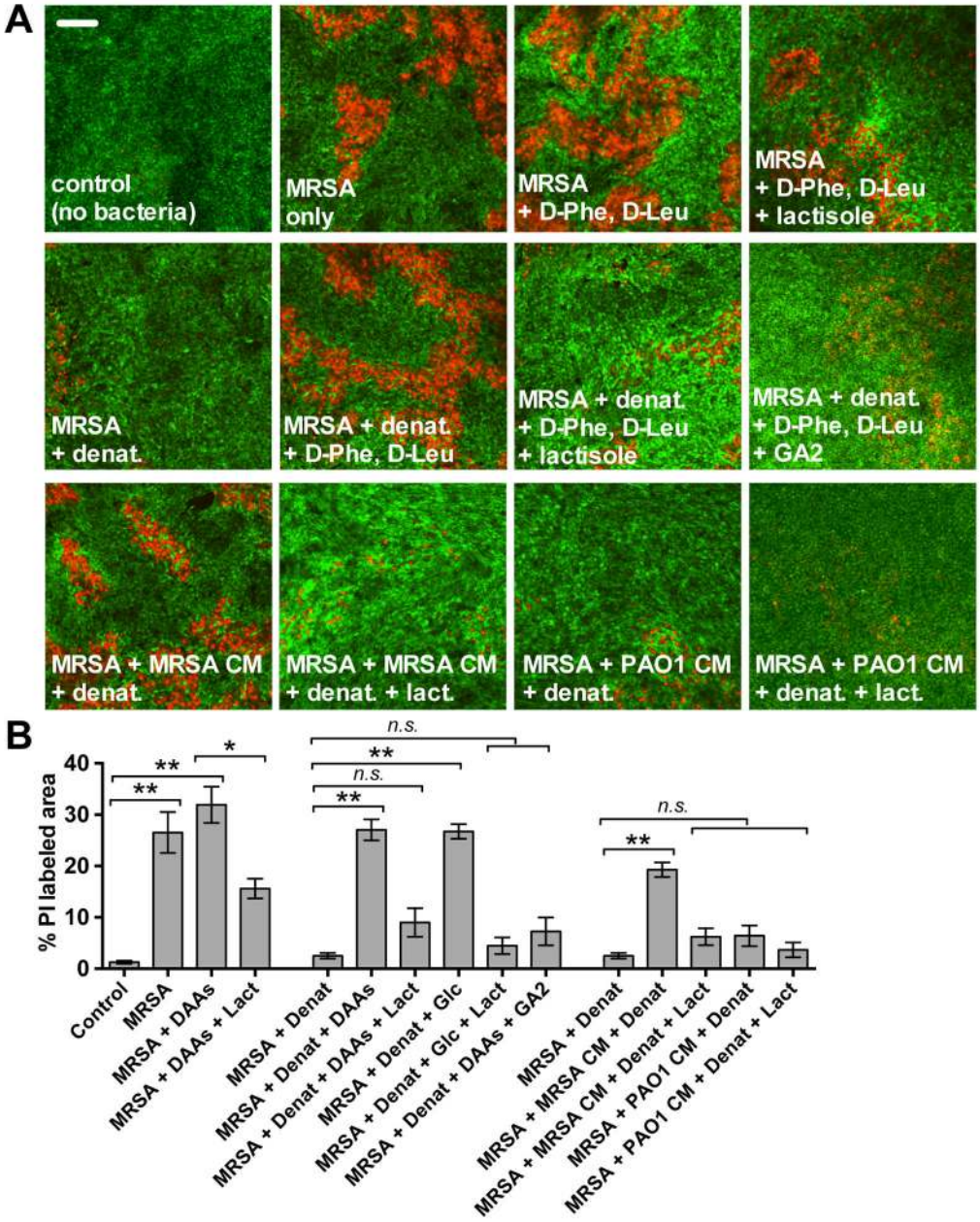

Fig. 5. Effects of D-amino acids on T2R-stimulated immune responses in vitro

(A) Representative images showing live cells labelled with Syto9 (green) and dead cells labelled with propidium iodide (red) in sinonasal ALI cultures after apical infection with MRSA in the presence or absence of D-Phe and D-Leu, lactisole, denatonium (Denat), gymnemic acid 2 (GA2), MRSA-conditioned medium (MRSA CM), or PAO-1–conditioned medium (PAO-1 CM) as indicated. N = 3–6 independent experiments for each condition, each experiment averaging 10 fields of view from 3 ALI cultures from the same patient. Scale bar, 100 μm. **(B)** Data from experiments as in panels A–B quantified as % propodium idodide (PI)–stained area. N = 3–6 independent experiments, each from a different individual patient) for each condition, with each experiment averaging 10 fields of view

from 3 ALI cultures from the same patient. Asterisks denote significance compared with the first bar of each graph (control conditions for that comparison) via one-way ANOVA with Dunnett's post-test; ** = p <0.01. All graphs show mean ± SEM (n = 4–6 patient ALI cultures for each condition).